Korean J. Chem. Eng., **14**(6), 469-473 (1997)

INFRARED SPECTROSCOPIC STUDY AND CHARACTERISTICS OF SnO_2-BASED THICK FILM FOR CH_3CN DETECTION

Jong Rack Sohn[†] **and Hyo Deck Park**

Department of Industrial Chemistry, Engineering College, Kyungpook National University, Taegu 702-701, Korea

(Received 22 September 1997 • accepted 26 November 1997)

Abstract – The $SnO_2/Al_2O_3/Nb_2O_5/SiO_2$ thick film devices were fabricated by screen printing and dipping methods, and their sensing characteristics to CH_3CN gas was investigated. The oxidation products of CH_3CN on the thick film were analyzed by FT-IR using a heatable gas cell. The IR results showed that the products formed by oxidation of CH_3CN at 300 °C on the $SnO_2/Al_2O_3/Nb_2O_5$ thick film without SiO_2 were mainly CO_2, H_2O, and NH_3, while on the $SnO_2/Al_2O_3/Nb_2O_5/SiO_2$ thick film products such as CO_2, H_2O, N_2O, HNO_3, and HNO_2 were observed. The thick film devices containing SiO_2 showed high selectivity and negative sensitivity to CH_3CN due to the presence of nitrogen compounds produced by oxidation of CH_3CN. Optimum amount of Nb_2O_5 and operating temperature were 1.0 wt% and 300 °C, respectively.

Key words: Oxidation of CH_3CN, SnO_2-based Sensor, FT-IR Spectra, Dipping of $Si(C_2H_5O)_4$, Negative Sensitivity

INTRODUCTION

Semiconductor gas sensors using SnO_2 and ZnO have been studied extensively since they were proposed by Seiyama et al. [1962]. These oxide gas sensors can detect various gases based the conductivity changes of their surface due to the adsorption and desorption of gases.

Successively, several research laboratories worked with the aim of developing new devices. The most recent research on flammable gas sensors has concentrated on SnO_2 in the form of thick-film and sintered ceramics [Lee et al., 1987; Torvela et al., 1988; Egashira et al., 1986]. The working mechanism of thick-film and sintered gas sensors is based on the build up of Schottky barriers between adjacent grains caused by the ionosorbed oxygen [McAleer et al., 1988].

The sensors show many advantages over optical or electrochemical sensors. The main advantages are their low cost, low consumption of electrical power, and high sensitivity. However, they should be improved due to a lack of stability and a poor selectivity.

An improvement of the selectivity of sensors based on SnO_2 is generally obtained by adding some specific catalysts such as Pd or Pt for heavy combustible gases [Torvela et al., 1991; Fryberger and Semancik, 1990; Klober et al., 1991], Bi_2O_3 for hydrogen [Sberveglieri et al., 1992], and ThO_2 for CO [Nitta and Haradome, 1979].

In this work, we have developed tin oxide-based thick film sensor for detection of acetonitrile gas which is known to be a poisonous chemical at low level in air. The sensing characteristics of SnO_2-based sensor to acetonitrile were studied by FT-IR analyses of gaseous species produced by oxidation of CH_3CN on the surface of sensor.

EXPERIMENTAL

Al_2O_3 (10.0 wt%) and Nb_2O_5 (0.2-2.0 wt%) were mixed mechanically with the base material, SnO_2, followed by calcination in air at 600 °C for 1 hr. The calcined sample was ground and then mixed with water to prepare paste. The paste was screen-printed onto an alumina substrate and then dipped into tetraethylorthosilicate solution followed by sintering in air at 700 °C for 1 hr. Fabrication flow chart of thick film

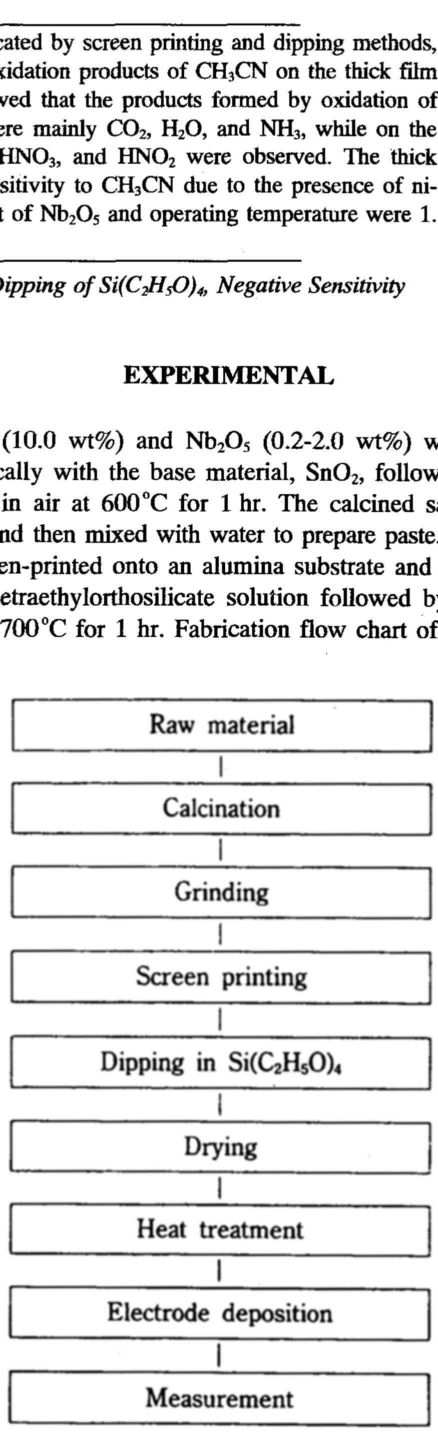

Fig. 1. Fabrication flow chart of thick film sensor.

[†] To whom all correspondence should be addressed.
E-mail: jrsohn@kyungpook.ac.kr

sensor for the detection of CH_3CN is given in Fig. 1. The sensor sensitivity was measured in a stainless box equipped with a heater, as described in a preceding publication [Park et al., 1993]. The sensitivity is defined as R_g/R_0, where R_0 and R_g are the electric resistances in fresh air and in the test gas, respectively. The products formed by reaction of CH_3CN on the surface of the sensor were analyzed by a Mattson Model GL 6030E FT-IR spectrometer using a heatable IR gas cell. FT-IR absorption spectra were measured over the range of 4,000-400 cm^{-1}.

RESULTS AND DISCUSSION

The optimum base material was selected based on the oxidation decomposition temperature of CH_3CN on the surface of various metal oxide and on the FT-IR analyses of the decomposed products. The decomposition reaction was carried out in a heatable gas IR cell under the condition of 20 torr CH_3CN and 500 torr air. The decomposition temperature of CH_3CN on metal oxides and their surface areas are listed in Table 1. On the surface of SnO_2, CH_3CN began to decompose at 130 °C and a lot of products were produced at 300 °C. The products from the decomposition reaction were H_2O, NH_3, CO_2, and N_2O. The easiness of decomposition on the surfaces of metal oxides falls in sequence:

$$SnO_2 > WO_3 > CoO > Fe_2O_3 > ZnO .$$

Fig. 2 shows the IR spectra of CH_3CN (16 torr) and the oxidation products of CH_3CN on SnO_2 thick film under the condition of CH_3CN 16 torr and air 16 torr at 300 °C for 0.5 hr. For pure CH_3CN, the bands at 2,967 and 2,940 cm^{-1} are assigned to CH_3 stretching vibration mode, while those at 1,444 and 1381 cm^{-1} are ascribed to the CH_3 deformation [Knoezinger and Krietenbrink, 1975]. The bands at 2,299 and 2,260 cm^{-1} are responsible for the CN group. However, on the SnO_2, the bands due to NH_3 and CO_2 in addition to CH_3CN were observed as shown in Fig. 2. The bands at 3,414, 1,624, 964, and 930 cm^{-1} are ascribed to the NH_3, while those at 3,723, 3,635, 2,361, and 667 cm^{-1} are due to the CO_2. Oxidation of CH_3CN on SnO_2 seems to proceed by the following reaction.

$$CH_3CN + 2O_2 = NH_3 + 2CO_2 \qquad (1)$$

Table 1. Decomposition temperature of CH_3CN on metal oxides and their specific surface area

Metal oxide	Type	Decomposition temperature (°C)	Surface area (m^2/g)
SnO_2	n	130	5.0
WO_3	n	150	4.4
CoO	p	200-220	4.5
TiO_2	n	230	6.1
Fe_2O_3	n	250	3.0
ZnO	n	>300	4.8

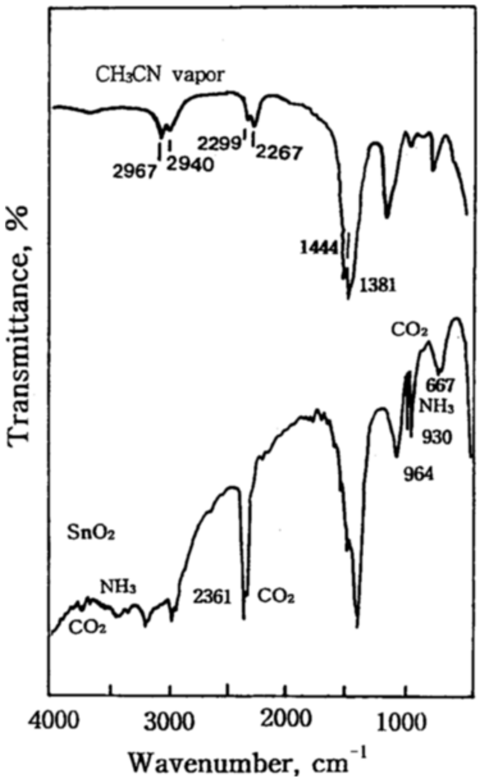

Fig. 2. Infrared spectra of CH_3CN and the oxidation reaction products of CH_3CN on SnO_2 thick film.

Fig. 3 shows IR spectra of oxidation products of CH_3CN on $SnO_2/Al_2O_3/Nb_2O_5$ and $SnO_2/Al_2O_3/Nb_2O_5/SiO_2$ at 300 °C for 0.5 hr. On $SnO_2/Al_2O_3/Nb_2O_5$, the bands (3,723, 3,635, 2,361, 667 cm^{-1}) due to CO_2 and the bands (3,414, 3,334, 964, 930 cm^{-1}) due to NH_3 were observed similarly to the case of SnO_2 in Fig. 2. However, on $SnO_2/Al_2O_3/Nb_2O_5/SiO_2$ thick film added with SiO_2, N_2O bands instead of NH_3 bands appeared at 2,238, 2,211, and 1,300 cm^{-1} [Nakamoto, 1997]. Also, the bands due the formation of nitrate or nitrite ions were observed at 1,381 and 1,358 cm^{-1} [Nakamoto, 1997]. N_2O seems to form by the oxidation of NH_3 produced by Eq. (1) as the follows.

$$2NH_3 + 2O_2 = N_2O + 3H_2O \qquad (2)$$

Also, for the IR absorption bands due to nitrate and nitrite groups, the following reaction is assumed to occur [Fonster and Lesine, 1978]

$$2NO_2 + H_2O = HNO_3 + HNO_2 \qquad (3)$$

Oxidation of CH_3CN on $SnO_2/Al_2O_3/Nb_2O_5$ thick film produced NH_3, as shown in Fig. 3. NH_3 oxidation was carried out in a gas cell to examine the behavior of NH_3 produced on the thick film, where the concentrations of NH_3 and air were 20 torr and 300 torr, respectively. The results are illustrated in Fig. 4. After reaction of NH_3 on $SnO_2/Al_2O_3/Nb_2O_5$ at 300 °C for 1 hr, other products except NH_3 were not detected, while at 350 °C the bands of H_2O (3,450 and 1,587 cm^{-1}) and N_2O (2,238, 2,211, doublet and 1,300, 1,273 cm^{-1} doublet) appeared. These results indicate that NH_3 is oxidized by the above Eq. (2) and the reaction occurs at 350 °C higher than 300 °C.

On the other hand, oxidation of NH_3 on $SnO_2/Al_2O_3/Nb_2O_5/SiO_2$ proceeded very easily even at 300 °C, as shown in Fig.

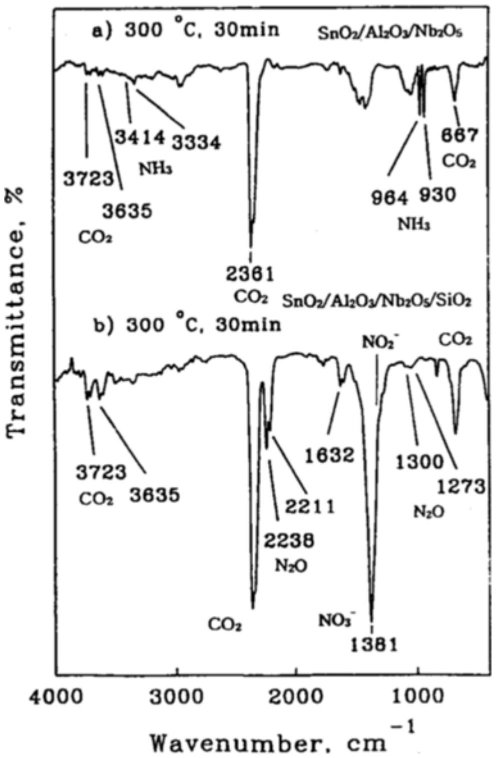

Fig. 3. Infrared spectra after oxidation reaction of CH_3CN on $SnO_2/Al_2O_3/Nb_2O_5$ (a) and $SnO_2/Al_2O_3/Nb_2O_5/SiO_2$ (b) at 300 °C for 0.5 hr.

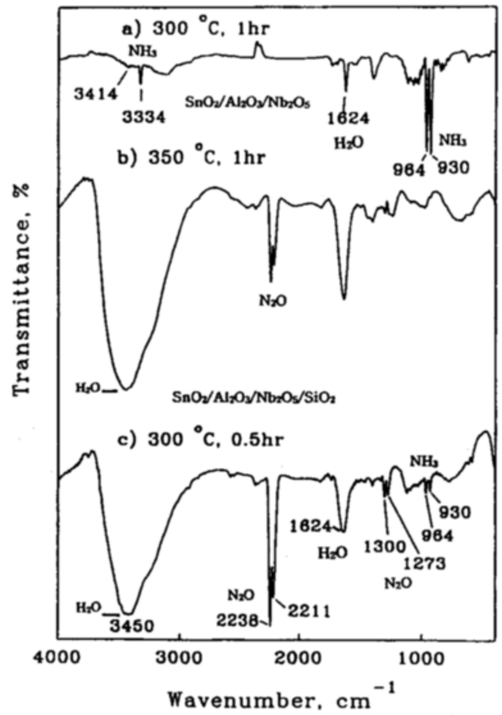

Fig. 4. Infrared spectra after oxidation reaction of NH_3 on $SnO_2/Al_2O_3/Nb_2O_5$ (a, b) and $SnO_2/Al_2O_3/Nb_2O_5/SiO_2$ (c).

4(c). Considering that the operating temperature of sensor is 300 °C, it is expected that addition of SiO_2 gives a significant effect on the characteristics and sensing selectivity of SnO_2 sensor.

Specific surface areas of some samples are listed in Table 2. The surface area of $SnO_2/Al_2O_3/Nb_2O_5/SiO_2$ is remarkably large compared to the other samples. It seems likely that the surface area also influences the sensing characteristics of sensor.

Fig. 5 shows infrared spectra of gases obtained by oxidation of CH_3CN on $SnO_2/Al_2O_3/Nb_2O_5/SiO_2$ at various temperatures for 0.5 hr, where the concentrations of CH_3CN and air are 20 torr and 300 torr, respectively. From room temperature to 160 °C, no bands except that of CH_3CN were observed, indicating that oxidation of CH_3CN did not occur. At 240 °C, bands due to CO_2 (2,361 cm^{-1}), N_2O (2,238, 2,211 cm^{-1}), HNO_3 (1,381 cm^{-1}), and HNO_2 (1,358 cm^{-1}) appeared and their intensities increased with reaction temperature as shown in Fig. 5. It is known that NH_3, CO_2, and H_2O increase the electric conductivity of sensor, while N_2O, HNO_3, and HNO_2 decrease the conductivity [Park et al., 1993]. Therefore, from the IR results of Fig. 5, it is clear that the SiO_2 component plays a great role in determining the detection limit of sensor.

Table 2. Specific surface areas of some samples

Sample	Surface area (m^2/g)
SnO_2	5.0
$SnO_2/Al_2O_3/Nb_2O_5$	22.0
$SnO_2/Al_2O_3/Nb_2O_5/SiO_2$	84.6

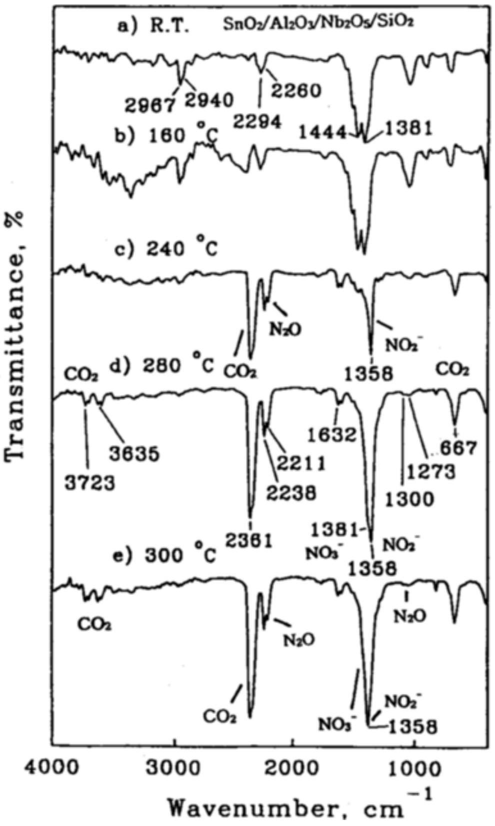

Fig. 5. Infrared spectra after oxidation reaction of CH_3CN on $SnO_2/Al_2O_3/Nb_2O_5/SiO_2$ at various temperatures for 0.5 hr.

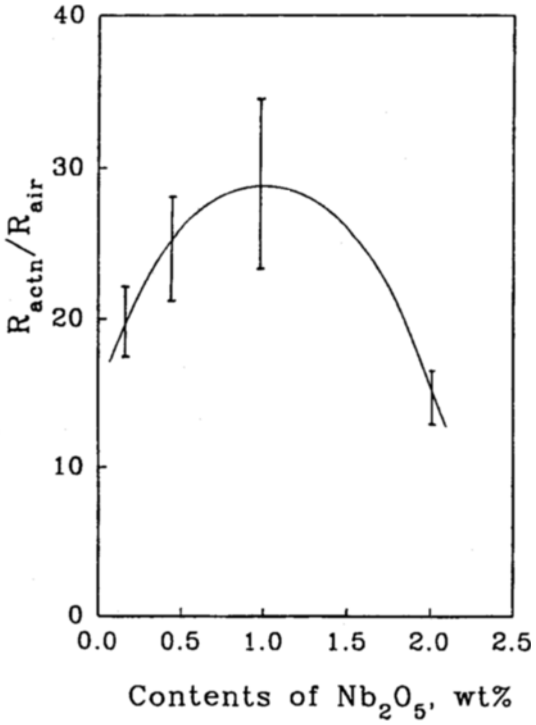

Fig. 6. Sensitivity of the $SnO_2/Al_2O_3/Nb_2O_5/SiO_2$ thick film device as a function of Nb_2O_5 content at 300 °C.

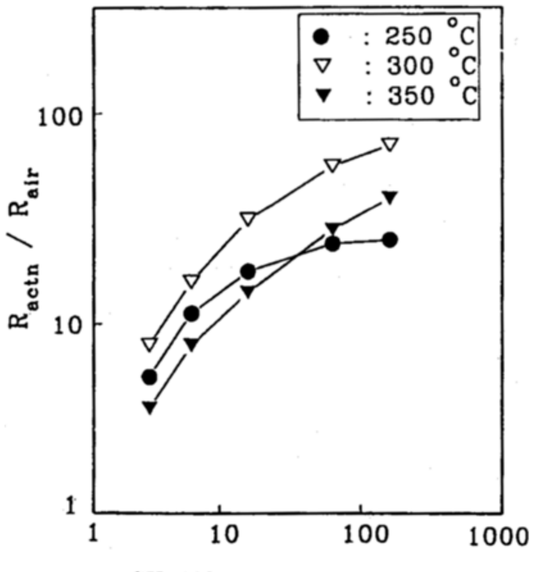

Fig. 7. Sensitivity of the $SnO_2/Al_2O_3/Nb_2O_5/SiO_2$ thick film device to CH_3CN at various operating temperatures.

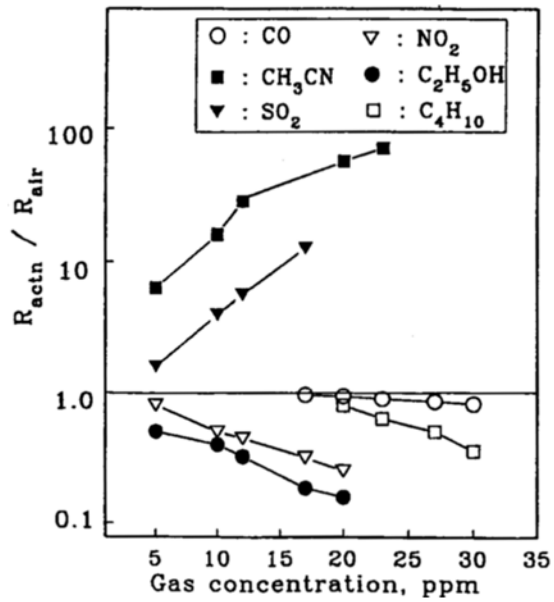

Fig. 8. Resistance characteristics of the $SnO_2/Al_2O_3/Nb_2O_5/SiO_2$ thick film device to various gases at 300 °C.

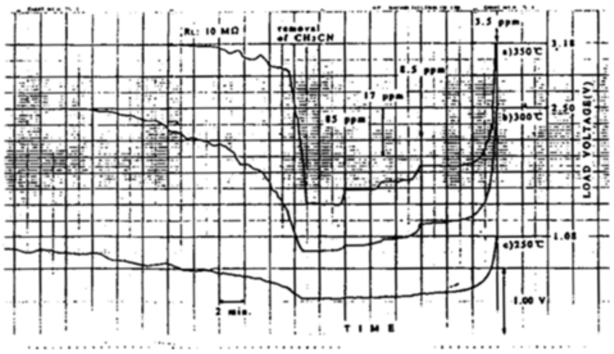

Fig. 9. Time responses of the $SnO_2/Al_2O_3/Nb_2O_5/SiO_2$ thick film device at different operating temperature.

We examined the dependence of N_2O_5 level (0.2-2.0 wt%) on the sensitivity of $SnO_2/Al_2O_3/Nb_2O_3/SiO_2$ sensor, when the concentration of CH_3CN was 17 ppm and the operating temperature was 300 °C. The $SnO_2/Al_2O_3/Nb_2O_5/SiO_2$ devices showed the negative sensitivity by increasing the resistance to CH_3CN, while the $SnO_2/Al_2O_3/Nb_2O_5$ devices without SiO_2 exhibited the positive sensitivity to CH_3CN. As shown in Fig. 6, the devices gave the highest sensitivity to 1.0 wt% N_2O_5, showing the increased resistance 22-35 times higher than for the devices with different content of Nb_2O_5 contents.

The sensing characteristics of $SnO_2/Al_2O_3/Nb_2O_5/SiO_2$ device are illustrated as a function of CH_3CN concentration at various operating temperatures in Fig. 7. The sensitivity increased with increasing the concentration of CH_3CN and the optimum operating temperature was 300 °C. It seems likely that the decreased sensitivity at 350 °C is responsible for the large formation of nitrogen compounds such as N_2O, HNO_3, and HNO_2 which decrease the electric conductivity, as shown in Fig. 5 [Park et al., 1993].

Fig. 8 shows sensing characteristic of $SnO_2/Al_2O_3/Nb_2O_5/SiO_2$ device to various gases at the operating temperature of 300 °C. The device exhibited the positive characteristic of decreasing the resistance to CO, NO_2, C_4H_{10} and C_2H_5OH, while the device exhibited negative characteristic of increasing the resistance to CH_3CN and SO_2. These results are in good agreement with the fact that, as shown in Fig. 3, $SnO_2/Al_2O_3/Nb_2O_5/SiO_2$ produce N_2O, HNO_3, and HNO_2 which decrease the electric conductivity of sensor [Park et al., 1993]. Therefore, the gas sensor shows high sensitivity and selectivity to CH_3CN.

Fig. 9 shows the response characteristics of the sensor to CH_3CN. The sensor was very sensitive to low gas concentration and the gas sensitivity tended to saturate in the range of high concentration (100 ppm). Also the sensor showed excellent recovery characteristics as the operating temperature increased. These results indicate that the response characteristics and sensitivity depend on the operating temperature. At 300 °C, the response and recovery times are 3 sec and 10 min, respectively.

CONCLUSIONS

The SnO_2-based thick film devices for the detection of CH_3CN were fabricated by the screen printing and dipping methods. The oxidation products of CH_3CN on $SnO_2/Al_2O_3/Nb_2O_5/SiO_2$ thick film were CO_2, H_2O, N_2O, HNO_3 and HNO_2. The oxidizing agents such as N_2O, HNO_3, and HNO_2 formed by oxidation of CH_3CN played an important role in determining sensitivity and selectivity to CH_3CN gas. The response time and the optimum operating temperature were 3 sec and 300 °C, respectively.

ACKNOWLEDGMENT

This work was supported by the Korea Science and Engineering Foundation through the Research Center for Catalytic Technology at Pohang University of Science and Technology.

REFERENCES

Egashira, M., Yoshida, M. and Kawasumi, S., "Gas Sensing Characteristics of Tin Oxide Whiskers", *Sensors and Actuators,* **9**, 147 (1986).

Foster, D. S. and Lesline, S. E., "Encyclopedia of Industrial Chemical Analysis", Interscience Ltd., New York, 1978.

Fryberger, T. B. and Semancik, S., "Conductance Response of $Pd/SnO_2(110)$ Model Gas Sensors to H_2 and O_2" *Sensors and Actuators, B,* **2**, 305 (1990).

Klober, J., Ludwig, M. and Schneider, H. A., "Effect of Thickness and Additives on Thin Film SnO_2 Gas Sensors", *Sensors and Actuators B,* **3**, 69 (1991).

Knoezinger, H. and Krietenbrink, H., "Infrared Spectroscopic Study of Adsorption of Nitriles on Aluminium Oxide", *J. Chem. Soc. Faraday Tran. 1,* **71**, 2421 (1975).

Lee, D. D., Sohn, B. K. and Ma, D. S., "Low Power Thick-Film CO Gas Sensors", *Sensors and Actuators,* **12**, 441 (1987).

McAleer, J. F., Mosely, P. T., Norris, J. O. W., Williams, D. E. and Tofield, B. C., "Tin Dioxide Gas Sensors", *J. Chem. Soc. Faraday Trans. 1,* **84**, 441 (1988).

Nakamoto, K., "Infrared and Raman Spectra of Inorganic and Coordination Compounds", A Wiley. Interscience Publication, John Wiley Sons, New York, 1978.

Nitta, M. and Haradome, M., "CO Gas Detection by ThO_2-Doped SnO_2", *J. Electron. Mater.,* **8**, 571 (1979).

Park, H. D., Cho, S. G., Sohn, J. R. and Lee, D. D., "Selectivity of SnO_2 Thick Film Gas Sensors Fabricated by Dipping into Tetraethylorthosilicate Solution to Acetonitrile", *J. Korean Sensor Soc.,* **2**, 17 (1993).

Sberveglieri, G., Groppelli, S., Nelli, P. and Camanzi, A., "A New Technique for Growing Porous SnO_2 (Bi_2O_3) Thin Films as Hydrogen Gas Sensors", *J. Mater. Sci. Lett.,* accepted for publication.

Seiyama, T., Kato, A., Fujiishi, K. and Nagatanui, M., "A New Detector for Gaseous Components Using Semiconductive Thin Films", *Anal. Chem.,* **34**, 1502 (1962).

Torvela, H., Romppainen, P. and Leppäuori, S., "Reduction of the Interference Caused by NO and SO_2 in the CO Response of Pd-Catalysed SnO_2 Combustion Gas Sensors", *Sensors and Actuators, B,* **4**, 479 (1991).

Torvela, H., Rompainen, P. and Loppävuori, S., "Detection of CO Levels in Combustion Gases by Thick-Film SnO_2 Gas Sensors", *Sensors and Actuators,* **14**, 19 (1988).